Available online at ScienceDirect

Nuclear Engineering and Technology

NUCLEAR ENGINEERING AND TECHNOLOGY
VOLUME 48, NUMBER 1

KOREAN NUCLEAR SOCIETY

Original Article

Nondestructive Testing of Residual Stress on the Welded Part of Butt-welded A36 Plates Using Electronic Speckle Pattern Interferometry

*Kyeongsuk Kim and Hyunchul Jung**[*]

Department of Mechanical System Engineering, Chosun University, 309 Pilmun-daero, Dong-gu, Gwangju 501-759, Republic of Korea

ABSTRACT

Most manufacturing processes, including welding, create residual stresses. Residual stresses can reduce material strength and cause fractures. For estimating the reliability and aging of a welded structure, residual stresses should be evaluated as precisely as possible. Optical techniques such as holographic interferometry, electronic speckle pattern interferometry (ESPI), Moire interferometry, and shearography are noncontact means of measuring residual stresses. Among optical techniques, ESPI is typically used as a nondestructive measurement technique of in-plane displacement, such as stress and strain, and out-of-plane displacement, such as vibration and bending. In this study, ESPI was used to measure the residual stress on the welded part of butt-welded American Society for Testing and Materials (ASTM) A36 specimens with CO_2 welding. Four types of specimens, base metal specimen (BSP), tensile specimen including welded part (TSP), compression specimen including welded part (CSP), and annealed tensile specimen including welded part (ATSP), were tested. BSP was used to obtain the elastic modulus of a base metal. TSP and CSP were used to compare residual stresses under tensile and compressive loading conditions. ATSP was used to confirm the effect of heat treatment. Residual stresses on the welded parts of specimens were obtained from the phase map images obtained by ESPI. The results confirmed that residual stresses of welded parts can be measured by ESPI.

Copyright © 2015, Published by Elsevier Korea LLC on behalf of Korean Nuclear Society.

1. Introduction

Residual stresses exist in materials and structures, independent of the presence of any external loads [1]. Most

manufacturing processes, including machining and welding, create residual stresses. For welding, the temperature field near the weld zone is changed by the moving heat source, leading to a nonuniform temperature distribution in the weld zone.

Fig. 1 – Speckle pattern on the image plane.

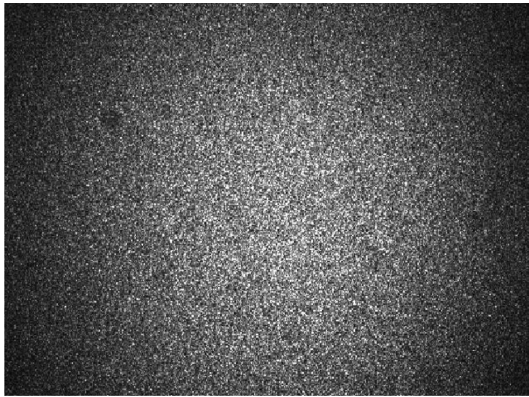Fig. 3 – MTS and ESPI system. ESPI, electronic speckle pattern interferometry; MTS, material test system.

Thermal expansion and contraction near the weld zone, due to the nonuniform temperature distribution, are constrained by the base material at low temperatures, which is located far from the weld zone. Finally, residual stresses are produced in the weld zone, including the heat-affected zone [2].

Residual stresses can reduce material strength and cause fractures. These stresses should be evaluated more precisely to estimate the reliability and aging of a welded structure. However, residual stress has been difficult to measure accurately. Heat treatment processes such as annealing, normalizing, and tempering can be used to relieve the locked-in stresses caused by welding. Annealing, in particular, is used to reduce residual stresses caused by welding so that a welded structure is not deformed or fractured. Annealing allows a welded structure to be heated at temperatures below the lower critical line (600–675°C for carbon steel). A welded structure is slowly heated for a sufficient period. It is then cooled uniformly throughout the cross-section and surface area [3].
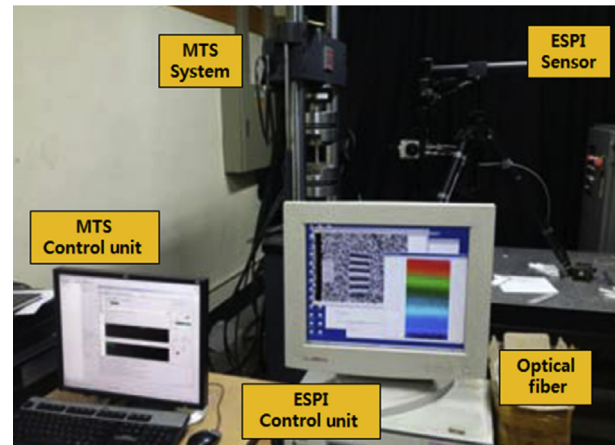
Many researchers have analyzed and measured welding-related residual stresses [1]. Hole drilling, ring coring, deep hole drilling, slitting, and contour methods are included in the category of destructive methods, while X-ray diffraction, neutron diffraction, magnetic, ultrasonic, and optical methods are included in the category of nondestructive methods. Optical techniques such as holographic interferometry, electronic speckle pattern interferometry (ESPI), Moire interferometry, and shearography are noncontacting methods used to measure residual stresses [4,5]. Among optical techniques, ESPI is typically used for measuring in-plane displacement such as stress and strain, as well as out-of-plane displacement such as vibration and bending, nondestructively.

Since ESPI is a noncontacting and nondestructive method, it does not need extra time for attaching strain gages or other
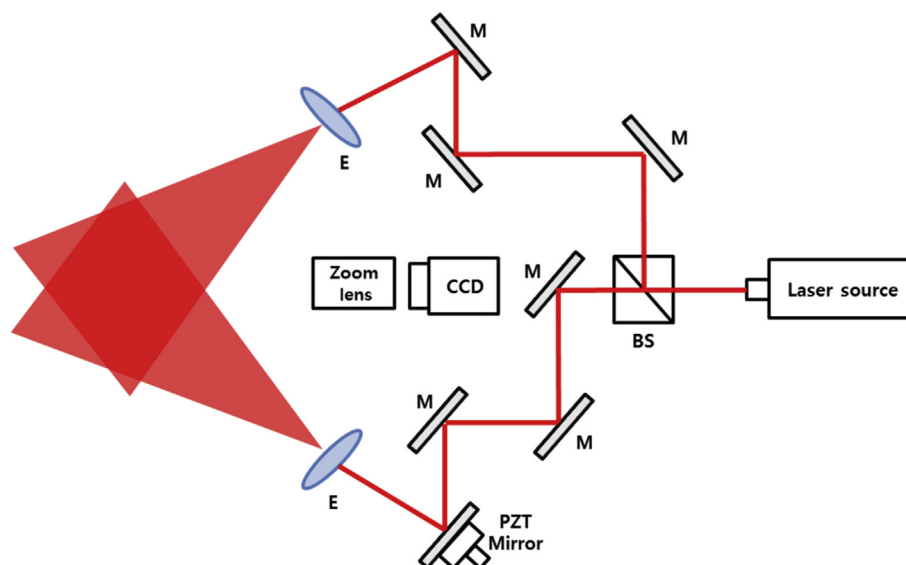

Fig. 2 – Schematic setup of in-plane displacement-sensitive ESPI. BS, beam splitter; CCD, charge-coupled device; E, expanding lens; ESPI, electronic speckle pattern interferometry; M, mirror; PZT, piezoelectric transducer.

Table 1 — Mechanical properties of ASTM A36.

Properties	Specification
Material	ASTM A36
Young's modulus	210 GPa
Poisson's ratio	0.26
Density	7,850 kg/m³

ASTM, American Society for Testing and Materials.

Fig. 5 — Load—displacement curve for base metal specimen.

devices for measuring the mechanical behavior of a welded structure. In addition, ESPI provides full-field data, which can provide information on an entire area where measurements were performed at a given time. With the phase shifting and phase unwrapping methods, ESPI can measure the amount of deformation quantitatively. Although it is a destructive method, the hole-drilling method is still used to measure residual stresses with ESPI. In some papers, the ESPI with hole-drilling method has been reviewed and compared with other measuring methods [6,7]. Min et al. [8] have developed a Moiré method with a hole-drilling method to determine residual stress and applied it to aluminum plates; Barile et al. [9] have analyzed the effects of parameters in residual stress measurements on titanium plates using ESPI with hole drilling.
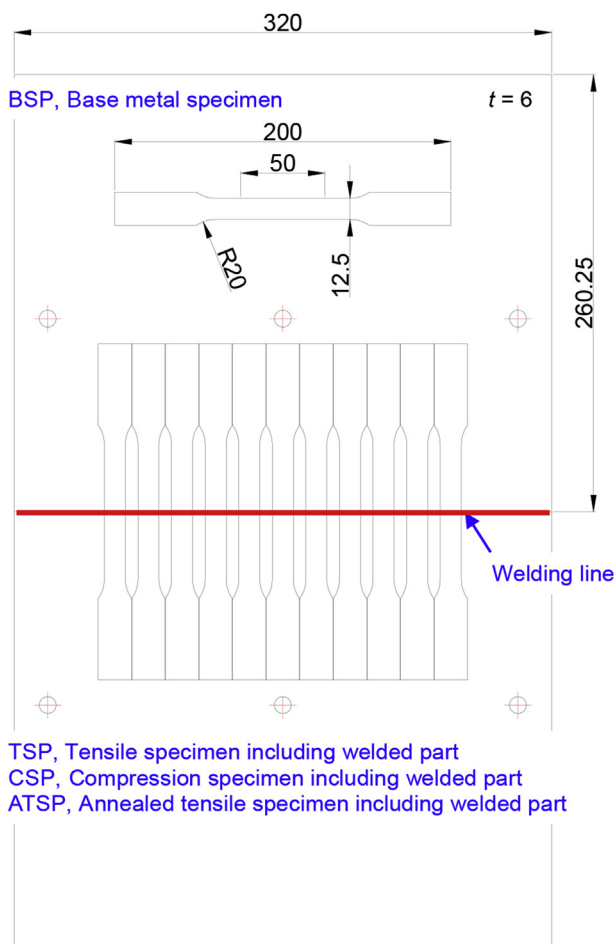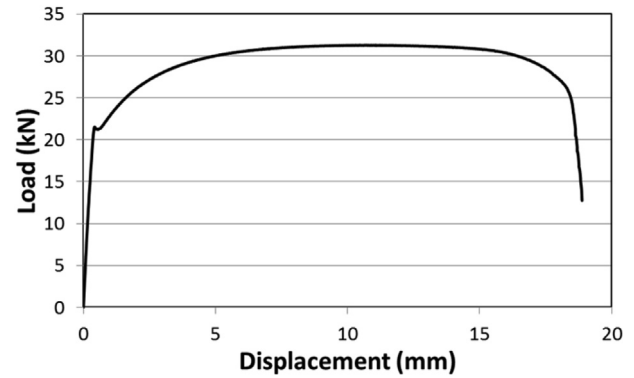
To measure the residual stresses of the welded parts of butt-welded American Society for Testing and Materials (ASTM) A36 plates, ESPI was used in this study. Two types of welded specimens were tested under tensile loading, while another type of specimen was tested under compressive loading. One of the tensile loaded specimens was annealed for 4 hours at 600°C. In order to know the elastic bandwidth of an A36 plate, a base metal specimen was tensile tested. Tensile loads of 3 kN, 4 kN, and 5 kN within the elastic bandwidth of A36 plate were selected. The result of the tensile tested specimen that was tested in a previous study [10] was

Fig. 4 — Schematic design of butt-welded specimen fabrication for tensile and compressive testing.
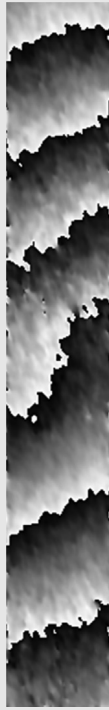
Table 2 — Phase map due to the difference of the tensile loading forces for BSP specimens using ESPI.

Loading force (kN)	3	4	5
Phase map			

BSP, base metal specimen; ESPI, electronic speckle pattern interferometry.

Table 3 – Phase map due to the difference of loading forces for TSP and CSP using ESPI.

Type of force	Tension (TSP)			Compression (CSP)		
Loading force (kN)	3	4	5	3	4	5
Phase map						

CSP, base metal specimen; ESPI, electronic speckle pattern interferometry; TSP, tensile specimen including welded part.

compared with that of the compressive tested specimen and also with that of the annealed tensile tested specimen.
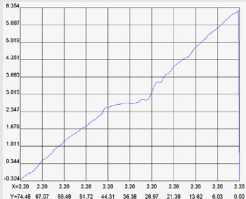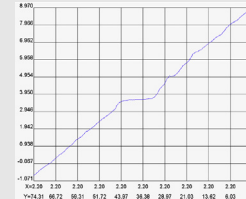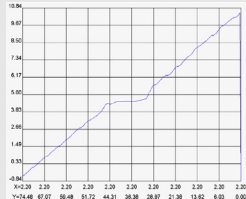
2. Materials and methods

2.1. Phase shifting ESPI

The surface of most materials is optically rough. When a laser light is illuminated on an object surface, it is scattered and/or reflected from the surface. Images of the object on the image plane are covered with a grainy structure, as shown in Fig. 1. This phenomenon is known as the speckle effect. Fig. 1 is an example of a speckle pattern on the image plane.

ESPI is one of the optical metrology methods that uses the speckle effect. ESPI uses this speckle effect to measure the deformation of an object and to analyze its behavior. More specifically, ESPI with an interferometer setup, which is more sensitive to an in-plane displacement, is used to measure the behavior of an object within its plane, such as strain and stress. Fig. 2 shows a schematic setup of the in-plane displacement-sensitive ESPI. The interferometer for the in-plane displacement-sensitive ESPI consists of a laser source (neodymium-doped yttrium aluminum garnet laser, 532 nm wavelength), a beam splitter, several mirrors, a beam expander, and a charge-coupled device camera with a zoom lens.
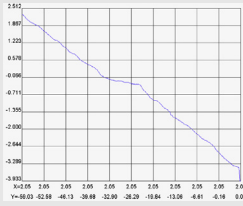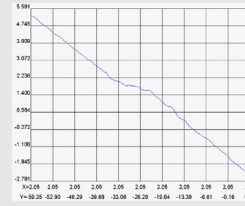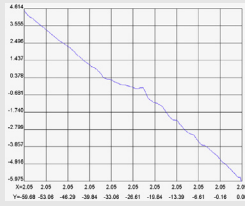
In order to measure the in-plane behavior of an object, an external force, such as tensile or compressive loading, vibration, thermal loading, etc., is applied to an object. While an

Table 4 – Line profile along the longitudinal center for the unwrapped phase data of TSP obtained by ESPI.

Tensile loading (kN)	3	4	5
Line profile			

ESPI, electronic speckle pattern interferometry; TSP, tensile specimen including welded part.

Table 5 – Line profile along the longitudinal center line for the unwrapped phase data of CSP obtained by ESPI.

Compressive loading (kN)	3	4	5
Line profile			

CSP, compression specimen including welded part; ESPI, electronic speckle pattern interferometry.

object is deforming, four-step phase shifting is applied and each image for each step taken by a charge-coupled device camera is stored into the computer memory. To obtain quantitative phase values of each point on the surface of an object, the phase shifting method is performed using a piezoelectric transducer, which is introduced in the reference laser beam path. The four-step phase shifting method is generally applied. Eq. (1) describes the intensity distribution of four images numerically [11].

$$I_1(x,y) = I_0(x,y)\{1 + \gamma \cos[\phi(x,y)]\}$$
$$I_2(x,y) = I_0(x,y)\left\{1 + \gamma \cos\left[\phi(x,y) + \frac{1}{2}\pi\right]\right\}$$
$$I_3(x,y) = I_0(x,y)\{1 + \gamma \cos[\phi(x,y) + \pi]\}$$
$$I_4(x,y) = I_0(x,y)\left\{1 + \gamma \cos\left[\phi(x,y) + \frac{3}{2}\pi\right]\right\}$$
(1)

where I_0 is the dc intensity, γ the modulation of the interference fringe, and $\phi(x,y)$ the wavefront phase. Then, the phase at each point on the surface of an object, which represents the status of an object before the deformation, can be calculated, as shown in Eq. (2):

$$\phi(x,y) = \tan^{-1}\left(\frac{I_4(x,y) - I_2(x,y)}{I_1(x,y) - I_3(x,y)}\right)$$
(2)

Another set of four-phase shifted images after deformation, obtained in the same manner, can be written as Eq. (3), and the phase after deformation can be calculated with Eq. (4):

$$I'_1(x,y) = I_0(x,y)\{1 + \gamma \cos[\phi(x,y) + \Delta\phi(x,y)]\}$$
$$I'_2(x,y) = I_0(x,y)\left\{1 + \gamma \cos\left[\phi(x,y) + \Delta\phi(x,y) + \frac{1}{2}\pi\right]\right\}$$
$$I'_3(x,y) = I_0(x,y)\{1 + \gamma \cos[\phi(x,y) + \Delta\phi(x,y) + \pi]\}$$
$$I'_4(x,y) = I_0(x,y)\left\{1 + \gamma \cos\left[\phi(x,y) + \Delta\phi(x,y) + \frac{3}{2}\pi\right]\right\}$$
(3)

$$\phi(x,y) + \Delta\phi(x,y) = \tan^{-1}\left(\frac{I'_4(x,y) - I'_2(x,y)}{I'_1(x,y) - I'_3(x,y)}\right)$$
(4)

where $\Delta\phi(x,y)$ is the phase change due to the deformation caused by an external force. Finally, this phase change can be obtained by subtracting Eq. (2) from Eq. (4).

2.2. Calculation of residual stress for butt-welded area

In order to measure the residual stress of the welded area of a butt-welded specimen with the ESPI system, a specimen is tested with a tensile or compressive loading force as an external force. For simplification of calculation, it was assumed that the residual stress of each point on the surface of the welded part, including the heat-affected zone and the melt area, is the same [10,12]. When the tensile or compressive loading is applied to a specimen, the deformation and strain that result are measured using ESPI.

First, the strain, Young's modulus, and stress of the base metal are obtained by ESPI and calculated numerically when tensile loading was applied to an A36 standard tensile testing specimen. Similarly, the strain, Young's modulus, and stress of
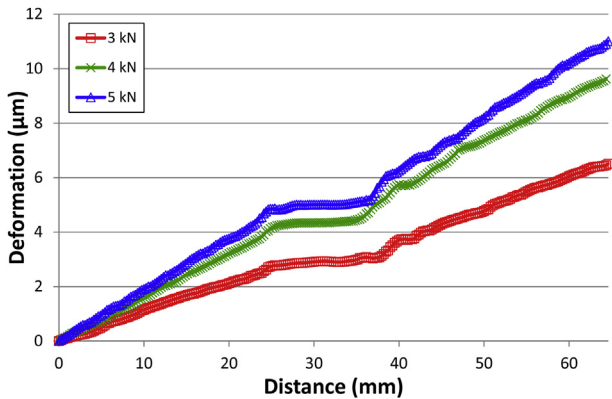
Fig. 6 – Comparison of deformation distributions along the longitudinal center line for tensile specimen.
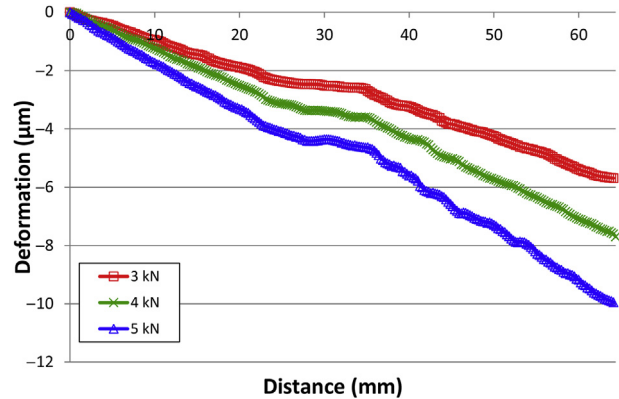
Fig. 7 – Comparison of deformation distributions along the longitudinal center line for compression specimen.

Table 6 – Numerical calculation results for TSP.

Tensile loading (kN)		3	4	5
Base metal	Cross-sectional area (m²)	7.50E−05	7.50E−05	7.50E−05
	Stress (MPa)	4.00E+07	5.33E+07	6.67E+07
	Deformation (μm)	1.09E+01	1.45E+01	1.81E+01
	Strain	1.91E−04	2.54E-04	3.18E−04
	Elastic modulus (GPa)	2.09E+11	2.10E+11	2.09E+11
Weld zone	Cross-sectional area (m²)	8.78E−05	8.78E−05	8.78E−05
	Stress (MPa)	3.42E+07	4.56E+07	5.69E+07
	Deformation (μm)	6.42E+00	1.00E+01	1.12E+01
	Strain	1.37E+04	2.14E+04	2.39E-04
	Elastic modulus (GPa)	2.50E+11	2.13E+11	2.38E+11

TSP, tensile specimen including welded part.

Table 7 – Numerical calculation results for CSP.

Compressive loading (kN)		3	4	5
Base metal	Cross-sectional area (m²)	7.50E−05	7.50E−05	7.50E−05
	Stress (MPa)	4.00E+07	5.33E+07	6.67E+07
	Deformation (μm)	1.05E+01	1.40E+01	1.75E+01
	Strain	1.91E−04	2.55E−04	3.18E−04
	Elastic modulus (GPa)	2.10E+11	2.10E+11	2.09E+11
Weld zone	Cross-sectional area (m²)	1.05E−04	1.05E−04	1.05E−04
	Stress (MPa)	2.86E+07	3.81E+07	4.77E+07
	Deformation (μm)	6.40E+00	8.50E+00	1.05E+01
	Strain	1.36E+04	1.81E+04	2.24E−04
	Elastic modulus (GPa)	2.10E+11	2.11E+11	2.13E+11

CSP, compression specimen including welded part.

the welded area of a butt-welded specimen are obtained by ESPI and calculated numerically when an A36 butt-welded tensile testing specimen underwent tensile and compressive loading.

The relationship of three parameters, the stress of the base metal σ_{base}, Young's modulus of the base metal E_{base}, and strain of the base metal ε_{base}, is written as Eq. (5). The residual stress included in the welded area, σ_{res}, is regarded as a part of the stress of the welded area of a butt-welded specimen, as shown in Eq. (6):

$$\sigma_{base} = E_{base} \cdot \varepsilon_{base} \tag{5}$$

$$\sigma_{rea} + \sigma_{base} = E_{weld} \cdot \varepsilon_{weld} \tag{6}$$

where E_{weld} is the Young's modulus of the welded area of a butt-welded specimen and ε_{weld} the strain of the welded area of a butt-welded specimen.

After substituting Eq. (5) for Eq. (6), σ_{res} is obtained as Eq. (7) [10]:

$$\sigma_{rea} = E_{weld} \cdot \varepsilon_{weld} - \sigma_{base} = E_{weld} \cdot \varepsilon_{weld} - E_{base} \cdot \varepsilon_{base} \tag{7}$$

Using a tensile testing system and ESPI, the strain, stress, and Young's modulus of the base metal and the welded area of a butt-welded specimen are measured without using any other methods.

2.3. Experiment

For measuring the residual stress of a butt-welded specimen, the material test system (Landmark System 370.10; MTS, Eden Prairie, Minnesota, USA) was used for tensile and compressive

testing, and the ESPI system (Q300; Dantec Dynamics, Skovlunde, Denmark) was used for measuring the deformation of a butt-welded specimen when tensile or compressive loading was applied to it, as shown in Fig. 3.

The welding process was carried out by an automatic CO_2 welding machine in order to keep the welding speed at a uniform 2 mm/s. In order to compare the residual stresses due to the welding states, the welding process was carried out with welding currents of 130 A, 140 A, and 150 A. The welding current of 140 A is associated with an optimal welding condition, while the current of 130 A results in an underwelded specimen and 150 A in an overwelded specimen. For securing a sufficient amount of the residual stress within the welded area, two butt-welded plates were fixed with a fixture on an automatic CO_2 welding machine during the welding process.

The butt-welded specimen was made of carbon structural steel (ASTM A36) plates. Table 1 shows the mechanical
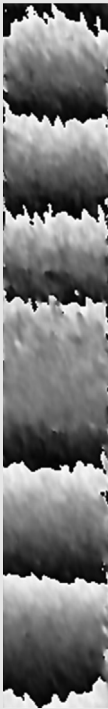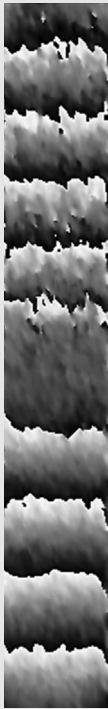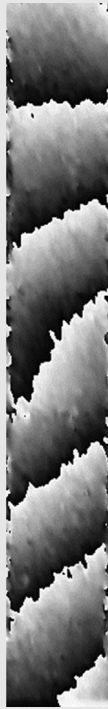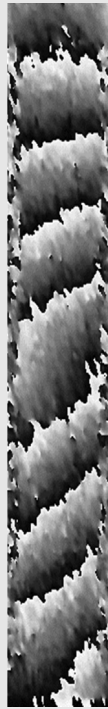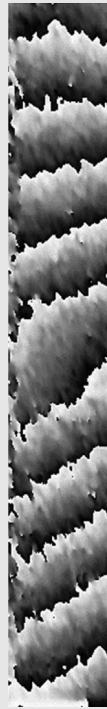
Table 8 – Residual stresses that remained in the weld zone of TSP and CSP, measured by ESPI.

Specimen	TSP	CSP
Loading force (kN)		
3	−5.83	−11.4
4	−7.78	−15.2
5	−9.72	−19.0

Unit for residual stress, MPa.
CSP, compression specimen including welded part; ESPI, electronic speckle pattern interferometry; TSP, tensile specimen including welded part.

Table 9 – Phase map due to the difference of the tensile loading forces for TSP and ATSP using ESPI.						
Heat treatment	Before annealing (TSP)			After annealing (ATSP)		
Loading force (kN)	3	4	5	3	4	5
Phase map						

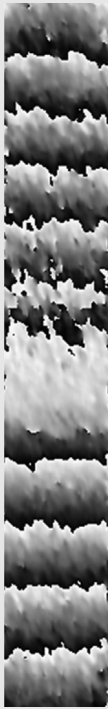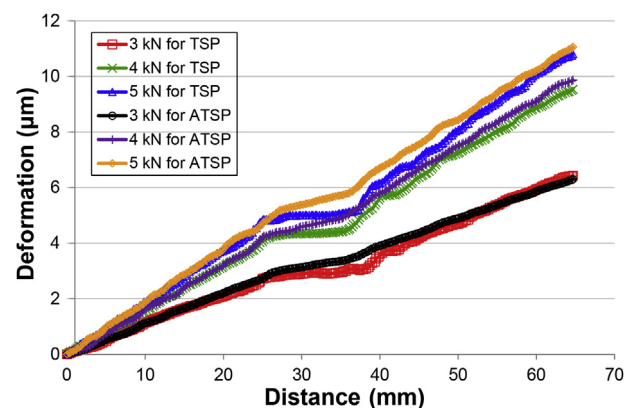ATSP, annealed tensile specimen including welded part; ESPI, electronic speckle pattern interferometry; TSP, tensile specimen including welded part.

properties of an A36 plate. In this study, four types of specimens (BSP, TSP, CSP, and ATSP) were prepared. Fig. 4 shows a schematic design of fabrication of four types of butt-welded specimens for tensile and compressive testing. All specimens were fabricated by the wire-cut electric discharge machining method. As shown in Fig. 4, the total length of a specimen is 200 mm, gage length is 50 mm, width is 12.5 mm, thickness is 6 mm, and radius of fillet is 20 mm. BSP is the standard tensile testing specimen of an original A36 plate [13]. TSP is the butt-welded specimen for tensile testing, while CSP is for compressive testing. ATSP is also a specimen for tensile testing, but it underwent heat treatment, unlike TSP. TSP, CSP, and ATSP include the welded area in the middle of a specimen.

BSP was used to obtain the load–displacement curve of an original A36 plate in order to select the loading condition. From the load–displacement curve, the elastic bandwidth of an A36 plate was verified, and then the tensile and compressive loading of 3 kN, 4 kN, and 5 kN within the elastic bandwidth were applied to other specimens for 30 seconds. TSP was compared to CSP and ATSP. TSP and CSP are the same specimens, but the applied loading forces are different. For TSP, the residual stress was calculated under the tensile loading condition, while it was calculated under the compressive loading condition for CSP. ATSP is the same as TSP, the only difference between them being that ATSP underwent heat treatment. After the tensile testing specimen was fabricated by wire-cut electric discharge

machining, the annealing process was applied to ATSP for 4 hours at 600°C.

During tensile and compressive testing, the deformation of a butt-welded specimen was measured by the ESPI system. The ESPI system set on an optical table is located in front of the material test system. The amount of deformation was obtained from a wrapped phase map image. After applying an unwrapping process, this wrapped phase map became an unwrapped one.

Fig. 8 – Comparison of deformation distributions along the longitudinal center line for TSP and ATSP. ATSP, annealed tensile specimen; TSP, tensile specimen.

Table 10 − Numerical calculation results for ATSP.

Compressive loading (kN)		3	4	5
Base metal	Cross-sectional area (m^2)	7.50E−05	7.50E−05	7.50E−05
	Stress (MPa)	3.98E+07	5.33E+07	6.68E+07
	Deformation (μm)	1.25E+01	1.64E+01	2.07E+01
	Strain	2.19E−04	2.88E-04	3.63E-04
	Elastic modulus (GPa)	1.82E+11	1.85E+11	1.84E+11
Weld zone	Cross-sectional area (m^2)	8.78E−05	8.78E−05	8.78E−05
	Stress (MPa)	3.59E+07	4.72E+07	5.90E+07
	Deformation (μm)	7.50E+00	1.15E+00	1.29E+01
	Strain	1.60E+04	2.45E+04	2.75E−04
	Elastic modulus (GPa)	2.25E+11	1.93E+11	2.15E+11

ATSP, annealed tensile specimen including welded part.

3. Results and discussion

Fig. 5 shows a load−displacement curve, which was obtained using the results of tensile testing of a BSP specimen. With this curve, the elastic bandwidth of A36 material was confirmed and 3 kN, 4 kN, and 5 kN of tensile and compressive loading forces were selected. For determining the elastic modulus of base metal, A36, tensile testing of BSP was carried out with 3 kN, 4 kN, and 5 kN of loading forces. From the results, the elastic moduli of the base metal specimen, BSP, were found to be 202 GPa, 205 GPa, and 204 GPa, respectively. Table 2 shows the phase map result obtained by ESPI. As shown in Table 2, as BSP was made of the A36 plate, interference fringes remained equidistant even though the number of fringes increased with an increase in the tensile loading force.

In general, the fringe pattern is usually formed parallel to the transverse direction. However, in this study, the fringe pattern was inclined. It seems that the specimen was clamped at a tilted angle, or the width ratio of the clamped part to the measured part of the specimen was small, because the fringe pattern tended to be parallel to the transverse direction when the width of the clamping part was longer than that of the measured part.

This study used the tensile testing results of TSP from a previous study [8]. For the comparison of results in accordance with the loading forces, CSP has been tested with a compressive loading force. Table 3 shows the phase map results due to the difference of loading forces for TSP and CSP using ESPI. Tables 4 and 5 show the line profiles along the longitudinal center line for the unwrapped phase data of TSP and CSP obtained by ESPI, respectively. The comparison results of the deformation distribution along the longitudinal center line for TSP and CSP are shown in Figs. 6 and 7, respectively.

In cases of both TSP and CSP, we can see that the slope of deformation was also increased when the loading force was increased. The slope of deformation for the welded part was lower than that of the base metal. Tables 6 and 7 show the results of the numerical calculations of the cross-sectional area, stress, deformation, strain, and elastic modulus of base metal and weld zone for TSP and CSP, respectively. The residual stress in the weld zone of TSP and CSP measured by ESPI was calculated using Eqs. (5−7), as shown in Table 8. At this time, the residual stress of CSP was double that of TSP. It seems that the residual stress of CSP acted as a compressive force in the weld zone.

Next, the evaluation of an annealing effect on the residual stress in the weld zone was carried out using an ATSP specimen. Table 9 shows the results of a phase map obtained by the difference of the tensile forces for TSP and ATSP using ESPI. A comparison of the results of the deformation distribution for TSP and ATSP is given in Fig. 8. It was found that the residual stress significantly decreased due to the heat treatment. As shown in Fig. 8, the slope of the weld zone of each specimen that underwent heat treatment approaches that of the base metal, because the residual stress was decreased by the heat treatment. Table 10 shows the results of the numerical calculations for ATSP. From these results, the residual stress in the weld zone for ATSP was calculated. As seen in Table 11, the residual stress was found to decrease quantitatively by the heat treatment. Residual stress with a negative value indicates that the weld zone is compressed under the tensile loading condition.

4. Conclusions

In this paper, the residual stress of the butt-welded specimen that was welded at a welding current of 130 A was measured by ESPI with a material test system. The result of the tensile test was compared with that of the compressive test. In addition, we compared the result of the tensile test before and after the heat treatment. Based on the results, we can make the following conclusions: (1) The residual stress obtained by compressive testing was about two times higher than that

Table 11 − Residual stresses that remained in the weld zone of TSP and ATSP, measured by ESPI.

Specimen	TSP	ATSP	Decreasing rate (%)
Loading force (kN)			
3	−5.83	−3.90	33.1
4	−7.78	−6.17	20.7
5	−9.72	−7.74	20.4

Unit for residual stress: MPa.
ATSP, annealed tensile specimen including welded part; ESPI, electronic speckle pattern interferometry; TSP, tensile specimen including welded part.

obtained by tensile testing. The reason for the residual stress of CSP to be higher may be that the residual stress of CSP acted as a compressive force in the weld zone; and (2) the residual stress after the heat treatment decreased slightly and was measured using ESPI quantitatively. The rate of decrease of the residual stress by heat treatment was 33.1% for 3 kN, 20.7% for 4 kN, and 20.4% for 5 kN.

The ESPI measurement technique is a useful nondestructive testing method for measuring the residual stress of a welded part.

Conflicts of interest

All contributing authors declare no conflicts of interest.

Acknowledgments

REFERENCES

[1] G. Schajer, Practical Residual Stress Measurement Methods, John Wiley & Sons, London, 2013.

[2] J.W. Park, Mechanism and effects of welding residual stress—mechanism of welding residual stress, J. KWS 22 (2004) 99−100.

[3] R. Singh, Applied Welding Engineering: Processes, Codes and Standards, Elsevier, Oxford, 2012.

[4] G.L. Cloud, Optical Methods of Engineering Analysis, Cambridge University Press, Cambridge, 1990, pp. 453−491.

[5] K.S. Kim, H.C. Jung, K.S. Kang, J.K. Lee, S.S. Jarng, J.K. Hong, In-plane strains measurement by using the electronic speckle pattern interferometry, KSME Int. J. 12 (1998) 215−222.

[6] X. Huang, Z. Liu, X. Huimin, Recent progress in residual stress measurement techniques, Acta Mech. Solida Sin. 26 (2013) 570−583.

[7] N.S. Rossini, M. Dassiti, K.Y. Benyounis, A.G. Olabi, Methods of measuring residual stresses in components, Mater. Des. 35 (2012) 572−588.

[8] Y. Min, M. Hong, Z. Xi, L. Jian, Determination of residual stress by use of phase shifting moiré interferometry and hole-drilling method, Opt. Lasers Eng. 44 (2006) 68−79.

[9] C. Barile, C. Casavola, G. Pappalettera, C. Pappalettere, Analysis of the effects of process parameters in residual stress measurements on titanium plates by HDM/ESPI, Measurement 48 (2014) 220−227.

[10] K.S. Kim, T.H. Choi, M.G. Na, H.C. Jung, Residual stress measurement on the butt-welded area by electronic speckle pattern interferometry, Nucl. Eng. Technol. 47 (2015) 115−125.

[11] K. Creath, Phase-shifting speckle interferometry, Appl. Opt. 24 (1985) 3053−3058.

[12] Apparatus for measuring residual stress and method thereof, Industry-Academic Cooperation Foundation, Chosun University, Korean Patent 10-1187408, 2012.

[13] ASTM, Standard Test Methods and Definitions for Mechanical Testing of Steel Products, Designation: A370-05, Annual Book of ASTM Standards, Vol. 01.03, West Conshohocken, ASTM International, 2006. pp. 91.